Enhancement of Oxidoreductase Cofactor Systems for Enzymatic Activity with 3'NADP: A Novel Model for NAD-capped RNA

Maria Russotti

Abstract:

Oxidoreductases working with their cofactors are the sole enzymes that catalyze the transfer of electrons from one molecule to another or to electrodes. Formate dehydrogenases are enzymes with considerable biotechnological potential as they can be used to produce optically active compounds from non-chiral ones. This is due to their strong stereospecificity in the transfer of hydride ion between the substrate and coenzyme. Oxidoreductase cofactor systems may also serve as an effective means for the enzymatic capture of CO_2. However, the separation of a cofactor from the enzyme is expensive and can cause harmful over purification, stunting the numerous biocatalysis reactions that could ensue. Recently discovered NAD-capped RNA in *Escherichia coli* can solve this issue of resupplying cofactors in oxidoreductase applications in a time-efficient, cost-effective manner. Cells naturally produce NAD-capped RNA, which can be sequestered inside the cells easily by expressing certain proteins known to naturally bind to them. For these capped molecules to be manipulated for in vitro and in vivo reactions, readily available 3' NADP served as a novel model for NAD-capped RNA because there is a parallel in their structures: a phosphate is attached in the same location in 3'-NADP as the RNA attaches in the NAD-capped RNA. In this study, formate dehydrogenase from *Candida boidinii* (CboFDH) was mutated through site-saturation mutagenesis, changing its cofactor specificity to demonstrate activity with 3'NADP, providing sufficient evidence for activity with NAD-capped RNA. The results from spectrometer enzyme assays indicated that two CboFDH mutants demonstrated increased activity with 3'NADP. Thus, the innovative use of 3'NADP in place of NAD-capped RNA demonstrated enzymatic activity with mutated CboFDH samples. This newfound information is the stepping-stone to more efficient use of oxidoreductases as biocatalysts and a maintainable process to limit excess CO_2 in the atmosphere.

Introduction:

Oxidoreductases are enzymes used in a wide range of applications. These include synthesis of chiral compounds, such as chiral alcohols, aldehydes and acids; preparation and modification of polymers, especially biodegradable or biocompatible polymers; biosensors for a variety of analytical and clinical applications; and degradation of organic pollutants [1].

Capture of CO_2 by employing enzymes provides a sustainable method to combat excess CO_2 overwhelming our environment today. The direct capture of carbon dioxide using enzymes such as formate dehydrogenase could be the ultimate carbon neutral process. There are no other known means for enzymatic capture of carbon dioxide currently available except for rubisco, as it is the primary tool for CO_2 capture in plants. The preliminary fixation of carbon dioxide in solution is extremely essential because once the gas is trapped, it can be fed into multiple one carbon metabolic pathways. Recently, immobilized nicotinamide adenine dinucleotide (NAD)-dependent formate dehydrogenase has been used to electrochemically reduce carbon dioxide to formate. The formate then can be enzymatically reduced to methanol, which is a functioning biofuel. The biofuel abilities are effective by utilizing NAD^+-dependent formaldehyde dehydrogenase and NAD^+-dependent alcohol [2]. These enzymes use the oxidation of their respective substrates, formate, formaldehyde, methanol, to produce NADH (Figure 1). The general approach is due to catalysts being able to facilitate both forward and reverse reactions equally, thus given excess of the product and sufficient reducing power, NAD^+-dependent dehydrogenases can reduce carbon dioxide to methanol.

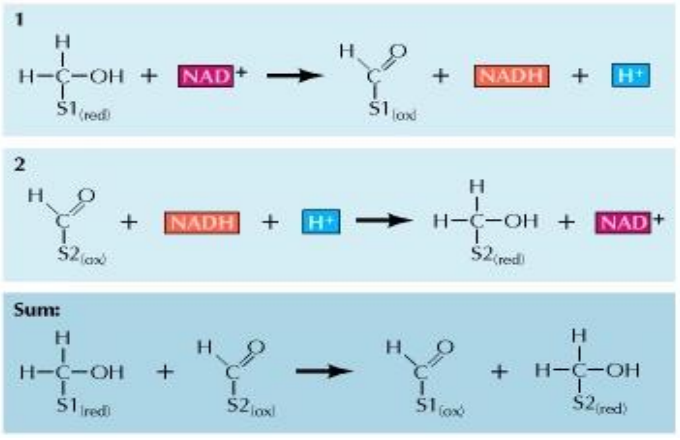

Figure 1: NAD^+ acts as a carrier of electrons in oxidation-reduction reactions by accepting electrons to form NADH (adapted from Cooper, Geoffrey M, 1970)

Cofactors are associated with oxidoreductases to facilitate their enzyme activity. However, if these enzymes can be used as biocatalysts you need an easy, inexpensive way to separate out its cofactor from its product. Additionally, over purification to separate the cofactor can lead to purifying out the enzyme entirely, which adds processing time and costs.

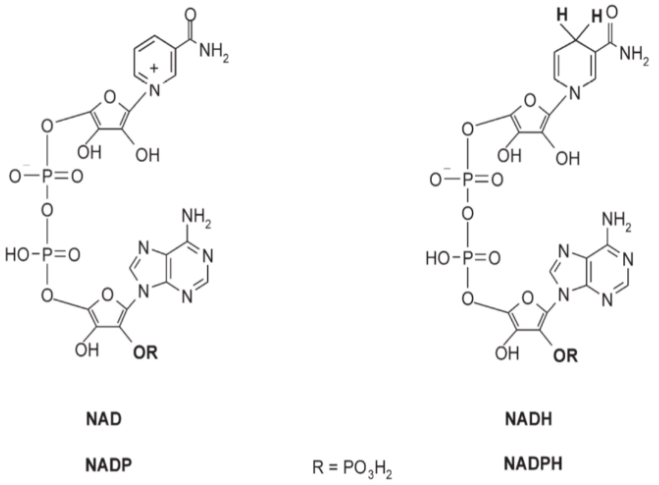

Figure 2: Structures of the cofactors NAD(P) and NAD(P)H (adapted from Vidal, Lara Sellés, et. al, 2017)

Most coenzymes such as NAD+, NADH, NADP, NADPH, as well as inorganic molecules like Zn^{+2} or Mg^{+2} have cofactors that are not permanently tethered to them. Figure 2 depicts NAD(P)(H) structures. Cofactors are essentially non-protein molecules the enzyme needs in order to be active. In the case of NAD(P)(H) when fastened to an enzyme, the cofactor needs to be supplied and replaced as the reaction proceeds. This makes the process very expensive, because oftentimes the cofactor is more expensive than the product being. For these reasons, there has been a great deal of interest in engineering of cofactor-based systems as the availability and the rate of regeneration of these native cofactors can easily become limiting, thus severely constraining the performance of both in vivo and in vitro bioprocesses [3].

In order to combat the harmful aspects in purification of the enzyme, non-living cells are utilized. These are regular whole cells which are permeabilized through their membranes using detergents or toluene. This process effectively kills the cells but leaves all the enzymes on the inside of the cell intact, successfully turning these cells into microreactors or “bags” for the enzymes. An obstacle in this method is keeping the cofactor sequestered in the interior, as the expensive cofactors can escape out of the permeabilized cells [4]. The recent discovery of E. coli and other prokaryotes producing a plethora of NAD-capped RNA molecules could provide a solution to this issue. In 2009, using high throughput liquid chromatography-mass spectrometry experiments, it was determined that prokaryotic cells contained small RNA molecules with

NAD(H) caps, which was unexpected at the time. These capped RNA molecules were found to be surprisingly abundant [5]**.** The amount of these capped RNA molecules can also be easily regulated by controlling the expression of an enzyme, in vitro and in vivo, called NudC. NudC is effective by being single-strand specific with a purine preference for the 5′-terminal nucleotide in RNA [6]. These NAD-capped RNA molecules are produced naturally by the cells, thus taking away the need to supply them. They also are sequestered inside the cells by expressing certain proteins that are known to naturally bind NAD-capped RNA.

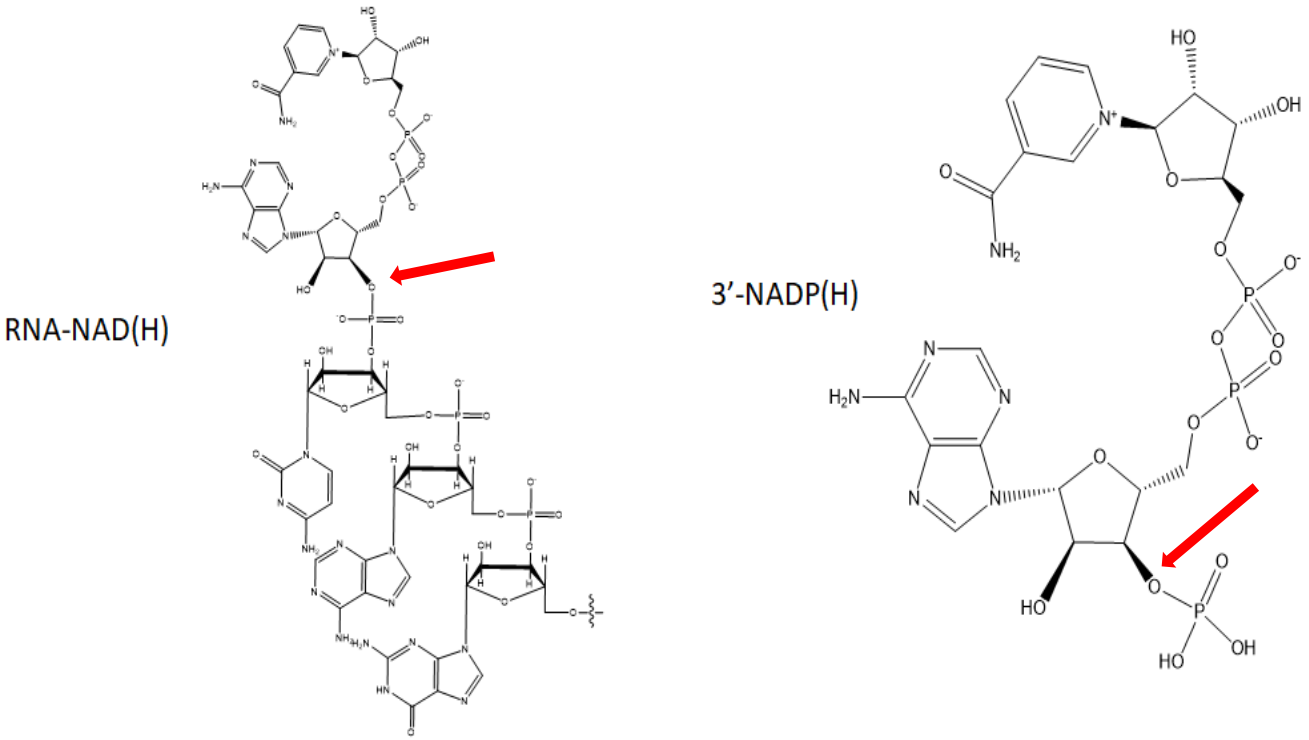

Figure 3: Structure of NAD-capped RNA vs. 3’NADP with red arrows indicating the phosphate attachment in 3’NADP and the RNA attachment in NAD-capped RNA.

The processes using this newfound NAD-capped RNA, can only be utilized if there are enzymes that can efficiently use NAD(H) modified with RNA at the 3’- position of the adenosine moiety. In order to test enzyme function with NAD-capped RNA, 3’NADP will be used as a substitute. 3’NADP is more readily available than NAD-capped RNA. Both are largely similar, with the phosphate attaching in the same spot in the 3'-NADP as where the RNA would attach in the NAD-capped RNA (Figure 3). Formate dehydrogenase from *Candida boidinii*

(CboFDH) is highly specific to NAD and virtually fails to catalyze with NADP. The reaction it catalyzes is exceedingly permanent. FDH is able to operate over a wide range of pH values, uses a cheap substrate, and methylotrophs provide a high scale enzyme production matrix for a relatively low cost, thus, making the enzyme a versatile catalyst [7]. The FDH enzyme is naturally able to use NAD(H) or NADP(H) as a cofactor. A principal determinant of coenzyme specificity for CboFDH is the structure is the loop region between beta-sheet 7 and alpha-helix 10 in the dinucleotide-binding fold that the cofactor is largely buried in the binding pocket of the protein, however the 2'- and 3'- positions are solvent exposed [8]. So, as a proof of concept, CboFDH that originally had no activity with 3'-NADP, will be transformed into mutated states.

The mutations can be produced through site-saturation mutagenesis. This allows for the incorporation of mutations into the plasmid by inverse PCR with standard primers. The primers can be designed in a back-to-back orientation and are effective with virtually any plasmid [9]. Based on previous sequence alignment with other formate dehydrogenases, two residues (Asp195 and Tyr196) may account for the observed coenzyme specificity in CboFDH [10]. Presence of negatively charged residues (aspartic, glutamic acid) in fingerprint GXGXXGX in beta-alpha-beta NAD binding region is critical for NAD+ dependent dehydrogenases [11]. In this way, a series of CboFDH mutants were developed and screened for their ability to utilize 3'NADP as a coenzyme.

Methods:

Organisms:

Formate Dehydrogenases from methylotrophic yeasts are easy to manipulate and are highly conservative. These yeasts are NAD dependent and have been used in developing NAD+ regeneration systems in organic synthesis for the production of added-value products. The FDH was extracted from live cultures of *Candida boidinii* and they were maintained

Resuspending CboFDH Gene Fragment:

A dried CboFDh gene (Sigma-Aldrich) was used and centrifuged for 5 seconds at 300xg. 100ul of ddH_20 was added to reach a concentration of 10ng/ul. The solution was incubated in 50^oC water for 20 minutes then, vortexed.

TOPO Cloning Reaction:

Using the TOPO cloning kit (ThermoFisher Scientific), pipette 2 ul of the resuspended CboFDH gene, 1 ul of TOPO salt solution, 2 ul of ddH_20, and 1 ul of TOPO vector into a PCR tube. Mix the reaction gently at room temperature, then store the reaction overnight at -20^oC.

Transforming TOPO reaction into DH5alpha:

DH5alpha *E.coli* cells are specifically engineered to have the greatest transformation efficiency. Before transformation, all materials including ligation products, cuvette, SOC media, and tips were pre-cooled for 10 min. Begin by thawing a vial of (C2987H) NEB alpha competent *E.coli* cells and thaw on ice for 10 minutes. Near a flame, add 2 ul of TOPO reaction product to a vial of competent cells and flick the tube 5 times to mix, then incubate on ice for exactly 30 minutes. Place the tube in a 42^oC water bath for 30 seconds. Place on ice for 5 minutes then, pipette 950 ul of room temperature SOC into the mixture and pipette mixture into a falcon tube. Place the falcon tube at 37^oC in a shaking incubator for 1 hour. The contents of the tube are spread onto LB-Kanamycin plates using glass beads and incubated overnight at 37^oC.

Analyzing TOPO-CboFDH clones:

Isolated colonies were chosen from the LB-Kanamycin plates in the TOPO reaction, to create bacterial overnights. These colonies were scraped into a falcon tube with 3ml TB along with 3 ul Kanamycin stock for the overnights. The following day 500 ul of each overnight was mixed individually with each 500 ul in a 2ml cryotube and placed in an -80^oC. The remainder bacteria was miniprepped. The overnights were spun down at 5000 rpm for 5-10 minutes and the supernatant was dumped. 250 ul of buffer P1 was added to each pellet and vortexed till the mixture was resuspended. Then, 250 ul of buffer P2 was added, capped the Eppendorf, and inverted 4-6 times to mix. Buffer N3 was added and mixed into solution by inverting 4-6 times.

The solution was centrifuged for 10 minutes at 13,000 rpm and the supernatant was pipetted into a spin column. The column was centrifuged for 1 minute and flow through was discarded. 750 ul of PE was added to the column, centrifuged and flow through was discarded, this step was done twice. The empty column was centrifuged for 4 minutes, and the tip from the spin column was then taken and placed in a new Eppendorf tube. 30 ul of warmed ddH20 was pipetted into the center of the filter, left standing for 1 minute, and centrifuged for 4 minutes at 13,000rpm. The concentration of the miniprepped samples were checked using nanodrop quantification and sent for DNA sequencing with the forward and reverse primers to confirm the gene was correct.

PCR amplification of CboFDH from TOPO-CboFDH

Forward and reverse primers for TOPO-CboFDH were diluted with ddH2O to create 10 mM solutions: adding 382 ul to the forward primer and 313 ul to the reverse primer. While PCR (polymerase chain reaction) was completing, an agarose gel was made to demonstrate the success of the PCR, using 10 ul of 1.0kB DNA ladder as DNA standard. Purple loading dye from BioLabs was used in each sample to stain the DNA for visibility. DNA, restriction digests and PCR products were visualized on a 1% (w/v) agarose gel in 1x TAE buffer (40 mM Tris acetate, pH 8.2, 1 mM EDTA). I then transformed the samples that showed successful cloning into DH5 alpha *E.coli* cells, using the same transformation method as previously discussed.

PCR linearization of pET-28a-TADH:

The linear sequence of FDH called for the complement of a linear pET-28a-TADH vector. After running general PCR protocol, the sample was subjected to Dpnl treatment. Since Dpnl cleaves only when a recognition site is methylated, restriction enzyme digestion was able to be performed with reliable restriction endonucleases.

Transformation into BL21(DE3) Competent Cells:

After proof of pET-28a linearization, the linear CboFDH was combined with the pET-28a to create a circular plasmid (pET28a-CboFDH). This was transformed into BL21 because for its key genetic markers and inducibility of protein expression. The BL21(DE3) competent cells

were from New England Biolabs. The bacteria were then grown on LB-kanamycin plates The following day the bacteria was miniprepped. An agarose gel was made to demonstrate the success of the PCR using 10 ul of 1.0kB DNA ladder as DNA standard. Purple loading dye from New England BioLabs (Ipswich, MA) was used in each sample to stain the DNA for visibility.

Site-saturation mutagenesis of CboFDH:

Six rounds of PCR were used to mutate six CboFDH mutants: D195A, D195N, D195Q, D195S, Y196H, and D195S-Y196H. They were then transformed into BL21 (DE3) competent cells. Hi-Fi DNA assembly Master Mix, Q5 site-directed mutagenesis kit, and E. coli BL21(DE3) expression cells were from New England Biolabs. The sequences of the mutagenic primers are given in Table 1.

Mutation	Forward primer	Reverse Primer
Asp195Asn (D195A)	TTT GTA TTA TAA CTA TCA AGC ATT GC	AGT TCC TTT GGA TTA AAT GG
Asp195Ser (D195S)	TTT GTA TTA TTC GTA TCA AGC ATT GCC TAA AG	AGT TCC TTT GGA TTA AAT GG
Asp195Ala (D195Q)	TTT GTA TTA TGC ATA TCA AGC ATT GCC	AGT TCC TTT GGA TTA AAT GG
Asp195Gln (D195N)	TTT GTA TTA TCA ATA TCA AGC ATT GCC	AGT TCC TTT GGA TTA AAT GG
Tyr196His (Y196H)	GTA TTA TGA CCA CCA AGC ATT GCC	AAA AGT TCC TTT GGA TTA AAT G
Asp195Ser/Tyr196His (D195S-Y196H)	TTT GTA TTA TTC GCA CCA AGC ATT GCC TAA AG	AGT TCC TTT GGA TTA AAT GG

Table 1: Each of the six mutations with their corresponding forward and reverse primer sequences

Mutation Analysis:

Samples of each of the six mutations were miniprepped and had each mutation concentration checked using nanodrop quantification. Samples of each mutation were then sent for DNA sequencing. Using Benchling, the sequence sent back of the mutated CboFDH were compared with the expected mutated sequences and garnered an average 98% match in sequence.

Expression of pET28a-CboFDH using IPTG:

The appropriate vectors containing the genes of interest were transformed into *E. coli* BL21(DE3) cells and plated on Luria-Bertani (LB) agar plates containing kanamycin. For the FDH seed culture, LB (50 ml) supplemented with antibiotic (100 μg/μl Amp for FDH-N or 50 μg/μl Kan for FDH-C) was inoculated with a single colony and incubated overnight at 37°C with shaking at 230 r.p.m. The seed culture (10 ml) was then diluted into LB (1 l) supplemented with antibiotic and the culture was grown at 37°C. When the culture reached an OD_{600} of ~0.6, isopropyl β-D-1-thiogalactopyranoside (IPTG) was added.

Purification of pET28a-CboFDH protein:

After the CboFDH was in frozen pelleted form, 40mM imidazole buffer was added aid in the resuspension of the pellet. Once thawed, the pellet was vortexed gently then sonicated. The sample was centrifuged for one hour at 7000xg. The supernatant from the sample after sonication was separated and kept for the column purification. 3ml of Ni-NTA resin (Clontech) was poured into a column and the manufacturers protocol was followed. The supernatant was applied onto the Ni-NTA column and washed with 2 column volumes (CV) of working buffer. Column was washed with 30 mM imidazole in working buffer to remove impurities. A supernatant, 0%, 5%,15%, 20%, 40% and 100% fractions well collected for each mutation and unmutated CboFDH from purification through the column. The fractions of the unmutated CboFDH were tested in a protein gel. A Novex Hi-density TBE sample buffer was used as a protein stain and Novex Sharp Pre-stained Protein Standard was used as a ladder.

Enzyme Activity Assays:

A multi-well plate was filled testing each of the CboFDH mutations. Using a SpectraMax M2 Spectrophotometer (Molecular devices) absorbance was monitored at 340 nm with a background absorbance at 800 nm. Enzyme activity was characterized in a NuPAGE MES SDS running buffer. Kinetic measurements were recorded every 20 seconds and change in absorbance at 340 nm was fit to a linear model. The following equation demonstrates how the specific

activity of the enzyme was calculated, where V_f is the final volume of the enzymatic assay and m_f is the mass (mg) of FDH enzyme [12]:

$$\text{specific activity} = \frac{\text{slope} * V_f}{6220 * m_f}$$

Well #	Protein Mutation	Protein (ul)	3'NADP (ul)	Formate (ul)	Buffer (ul)
1	D195A	6.49	5	5	183.51
2	D195N	6.33	5	5	183.67
3	D195Q	17.24	5	5	172.76
4	D195S	15.87	5	5	174.13
5	Y196H	4.83	5	5	185.17
6	D195S-Y196H	6.58	5	5	183.42
7	NONE	0	5	5	190

Table 2: Contents of the wells in the activity assay that tested the CboFDH mutants

Results:

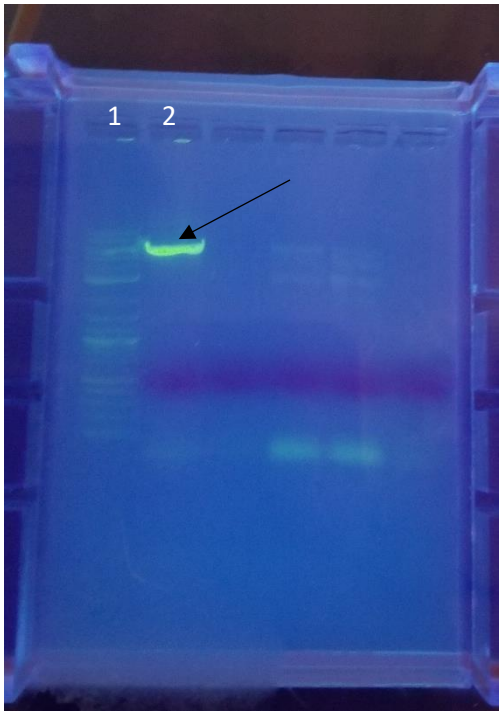

Figure 4: Well 1 contains the 1kb plus Ladder (BioLabs). Well 2 shows a fluorescent band at approximately 6 kb, which is the correct size for the linearized pET-28a.

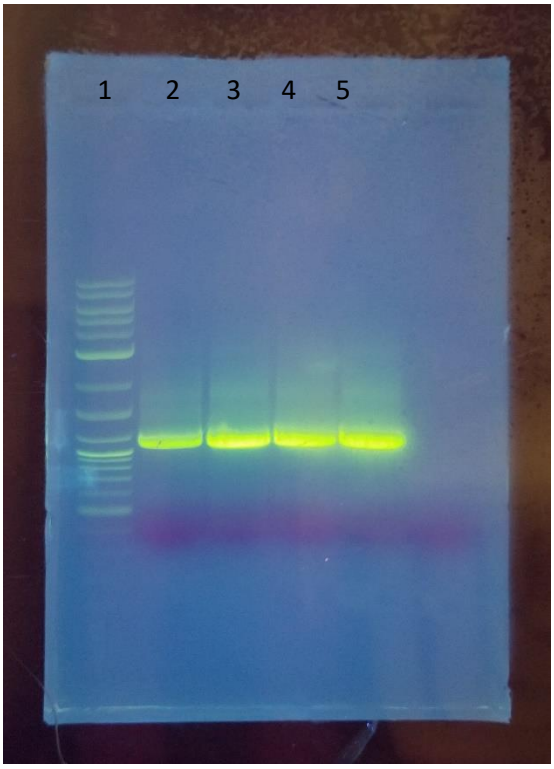

Figure 5: Well 1 contains the 1kb plus Ladder (BioLabs). Wells 2-5 show a fluorescent band at 1kb, which is the distance of the plasmid.

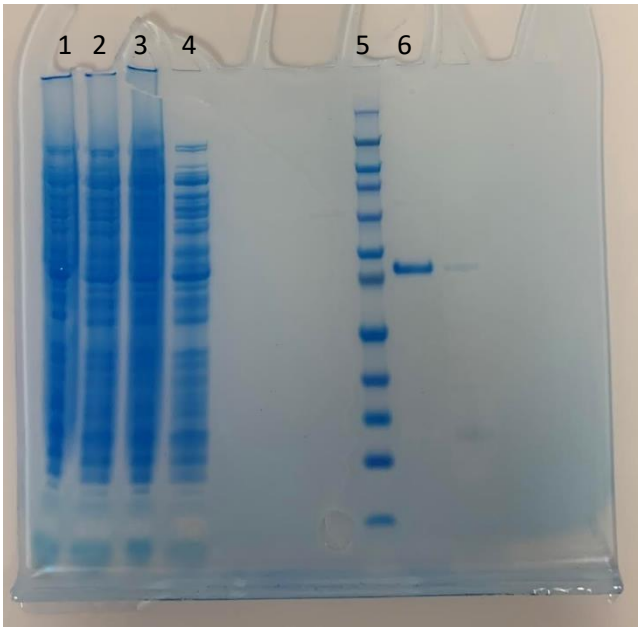

Figure 6: Well 5 contains Novex Sharp Pre-stained Protein Standard ladder. In well 6, the 40% fraction of CboFDH was tested and shows approximately 45 kDa, the molecular weight of CboFDH. Wells 1-4 contained 5%,15%, 20%, and 100% fractions respectively, but did not show adequate bands.

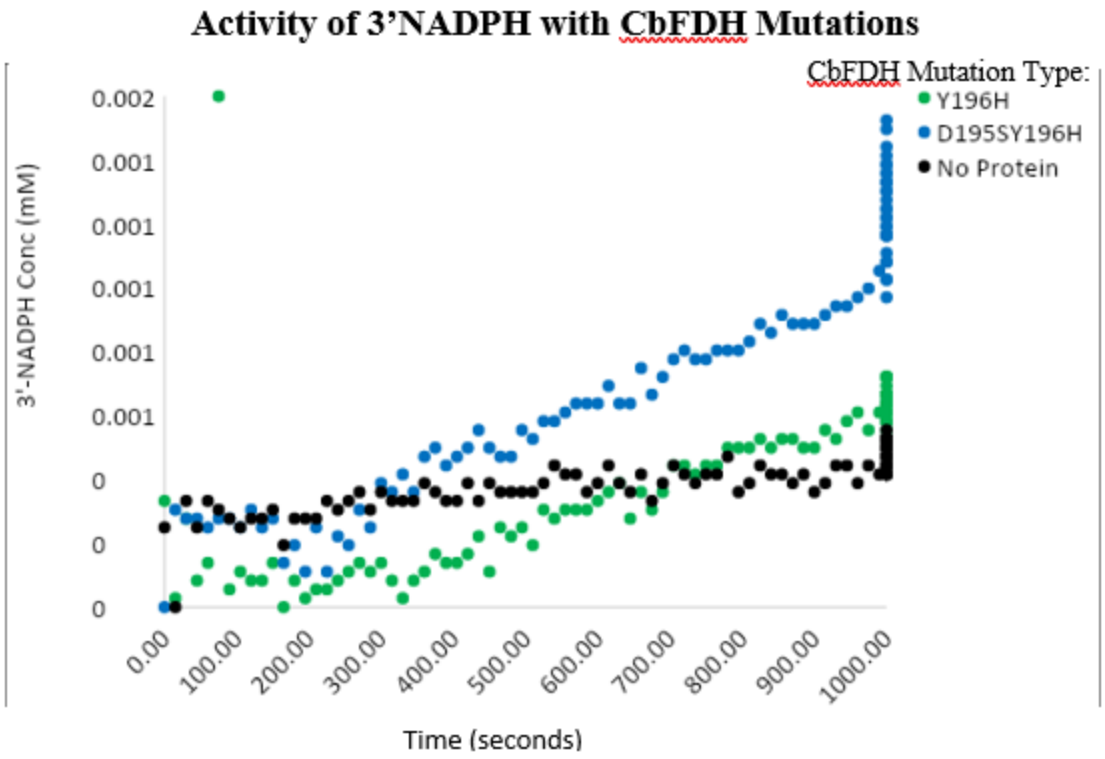

Graph 1: Activity assay graph showing activity of two CboFDH mutants (Y196H and D195S-Y196H) with 3'NADP. The two mutants demonstrated increased absorbance compared to the control with no protein.

Discussion:

The *E.coli* genome does not contain the formate dehydrogenase gene. The transformation of the gene into DH5alpha, competent *E.coli* cells, was to make the bacteria gain the TOPO vector. This transformation was using TOPO and DH5alpha (strain of *E.coli*) was the most productive method to insert a formate dehydrogenase gene in *E.coli*. This was done with general transformation procedures and grown on LB Kanamycin plates. These bacteria were then distinguished into select colonies and made into overnights and set in the shaking incubator at 180 rpm. For analysis of the TOPO-CboFDH clones, colony selection from the plates was done by choosing isolated colonies. Any colonies too close to each other may cause risk of cross contamination. Following the bacterial miniprep of the TOPO-CboFDH, concentrations were tested using a spectrophotometer Nanodrop. Knowing the concentrations in each sample, the adequate amount of bacterial product was able to be sent out for sequencing results. PCR linearization of pET-28a-TADH became vital to serve as a complement to the linear CboFDH

gene in the *E.coli* bacteria. The location of affinity tags in the sequence of CboFDH can interfere with enzymatic activity, thus the FDH gene was cloned into the pET28a vector to obtain a protein C-terminal His_6-tag. Success of the pET-28a-TADH PCR was proven by the through the clear bands in the gel (Figure 4). The base pair length of the band, approximately 6 kb, proved to be the same length of the linearized pET-28a-TADH. With these two linear aspects ready for blending, the linear CboFDH was combined with the pET-28a to create a circular plasmid (PET28a-CboFDH). These plasmids were then able to be transformed into BL21 (DE3) Competent *E. coli*. BL21 *E.coli* are widely used in T7 expression. When put onto LB Kanamycin plates there was a high yield of colonies.

Six mutations were directed into the CboFDH with six rounds of PCR and miniprep. The success of the mutations with Asp195 come from the fact that Asp195 conserved residue, interacts with 2' and 3'-OH of adenosine ribose. Additionally, mutations with Tyr196 were enacted because having a tyrosine in 196 position, is only conserved in yeast and fungi enzymes. This is located at the entrance of the coenzyme binding site and could prevent NADP binding either by unfavorable interactions or by sterically blocking the 2'-phosphate group binding. Comparison of the mutated DNA to the exact sequence of each mutation proved to have an approximately 98% overlap. With the success of the site-saturation mutagenesis, the CboFDH was expressed with IPTG to garner greater protein production. In the purification of the pET-28a-CboFDH protein, washing through the Ni-NTA column of the supernatant, 5%, 10%, 15%, 20%, 40% and 100% imidazole buffer solutions were tested. The 40% solution expressed the pET-28a-CboFDH protein most clearly which was visualized in a well-defined protein band (Figure 6). Therefore, the 40% fraction was used in further testing. All six prepared Cbo-FDH mutations were tested in a spectrometer activity assay with 3'NADP. Multi-well plates were filled with 40 mM 3'NADP, formate, buffer, and the respective CboFDH protein. The control well had all other components, instead of the protein it included additional buffer. After running the spectrometer at an absorbance of 340 nm, collected data every 20 seconds, two mutants indicated activity with 3'NADP compared to the control. Based upon the spectrometer activity assay it can be proven that the Y196H and D195S-Y196H CboFDH mutants provide a suitable protein for the 3'NADP cofactor (Graph 1).

Conclusion:

My research was able to establish successful activity of CboFDH mutants with 3'NADP, subsequently providing evidence of activity with NAD-capped RNA. Previous research indicated that for certain formate dehydrogenases to have NADP dependence, their sites were typically occupied by hydrophobic residues. There is a need for charged amino acid residues at the binding site of 2'-phosphate group of $NADP^+$ for charge stabilization and an increased space in the binding site [13]. However, the dependence of FDH with 3'NADP had not been thoroughly explored.

In this study, CboFDH was subject to site-saturation mutagenesis and then evaluated for enzymatic activity with 3'NADP. The successful transformations of CboFDH and linearized pET-28a allowed for the creation of the plasmid pET28a-CboFDH. Through a series of site-saturated mutations, expression, and purification, the CboFDH was then able to be tested with activity 3'NADP. Mutations Y196H and D195S-Y196H demonstrated enzymatic activity with 3'NADP in the spectrometer assay.

Further research will be conducted with the two effective CboFDH mutants with NAD-capped RNA. The activity of the two mutants with 3'NADP indicates a probable efficacy with the mutants and NAD-capped RNA. This is because 3'NADP was a model for the capped RNA, both having structural similarities. The short shelf life of 3'NADP caused limitations in the number of activity assay trials; so, additional assays should be conducted. If imminent studies with these mutants and NAD-capped RNA are effective, this will be a clear solution to the current drawbacks of oxidoreductases. Thus, providing a remedy for the need to resupply expensive cofactors in oxidoreductase cofactor systems.

Consequently, this study successfully created CboFDH mutants with the ability to be active with a newfound cofactor model: NAD-capped RNA. These results will be a foothold in developing highly efficient oxidoreductase applications. From the enzymatic conversion of carbon dioxide to implementations in modern medicine, the CboFDH mutants in this study provide a basis to essential applications.

Bibliography:

1. Sheldon WM, Stephen RP. Oxidoreductase enzymes in biotechnology: current status and future potential. Bio/Technology 1983;1:677–86.

2. Kim Y.H., Campbell E., Yu J., Minteer S.D. and Banta S. (2013) Angew. Chem. Int. Ed., 52, 1437–1440. [PubMed] [Google Scholar]

3. Liu, Wenfang, and Ping Wang. "Cofactor Regeneration for Sustainable Enzymatic Biosynthesis." *Biotechnology Advances*, vol. 25, no. 4, July 2007, pp. 369-84, doi:10.1016/j.biotechadv.2007.03.002.

4. Rasmussen, R.E., Erstad, S.M., Ramos-Martinez, E.M. *et al.* An easy and efficient permeabilization protocol for in vivo enzyme activity assays in cyanobacteria. *Microb Cell Fact* **15,** 186 (2016) doi:10.1186/s12934-016-0587-3

5. Munafo, D.B., Robb, G.B.2010.Optimization of Enzymatic Reaction Conditions for generating representative pools of cDNA from small RNA. RNA 16: 2537–2552

6. Höfer, Katharina, et al. "Structure and Function of the Bacterial Decapping Enzyme NudC." *Nature*, vol. 12, 18 July 2016, pp. 730-34, doi:10.1038/nchembio.2132.

7. Mozzanega, Philippe. *Characterisation of the Enzymes Involved in Methanol Dissimilation in Bacillus Methanolicus Assessment of Enzyme-based Biohydrogen Production for a Cell-free Biofuel Cell*. 2010. U of Bath, PhD thesis. pdfs.semanticscholar.org/b28a/ca67fc1e414ecbe12e1c4b26ad7b287b374d.pdf.

8. Andreadeli, Aggeliki, et al. “Structure-Guided Alteration of Coenzyme Specificity of Formate Dehydrogenase by Saturation Mutagenesis to Enable Efficient Utilization of NADP+.” *FEBS Journal*, vol. 275, no. 15, 2008, pp. 3859–3869., doi:10.1111/j.1742-4658.2008.06533.x.

9. Biolabs, New England. “Site Directed Mutagenesis.” *NEB*, www.neb.com/applications/cloning-and-synthetic-biology/site-directed-mutagenesis.

10. Bubner, Patricia, et al. “Structure-Guided Engineering of the Coenzyme Specificity OfPseudomonas Fluorescensmannitol 2-Dehydrogenase to Enable Efficient Utilization of NAD(H) and NADP(H).” *FEBS Letters*, vol. 582, no. 2, 2007, pp. 233–237., doi:10.1016/j.febslet.2007.12.008.

11. Deng, Win Ping, and Jac A. Nickoloff. “Site-Directed Mutagenesis of Virtually Any Plasmid by Eliminating a Unique Site.” *Analytical Biochemistry*, Academic Press, 29 Nov. 2004, www.sciencedirect.com/science/article/pii/000326979290280K.

12. Takacs, Michelle, et al. “Secretion of Functional Formate Dehydrogenase in Pichia Pastoris.” *Protein Engineering, Design & Selection : PEDS*, Oxford University Press, 1 Mar. 2017, www.ncbi.nlm.nih.gov/pmc/articles/PMC6075411/.

13. A. Andreadeli, D. Platis, V. Tishkov, V. Popov, N.E. Labrou, FEBS J. 275 (2008)

    3859–3869.

14. Cooper, Geoffrey M. “The Central Role of Enzymes as Biological Catalysts.” *The Cell: A Molecular Approach. 2nd Edition.*, U.S. National Library of Medicine, 1 Jan. 1970, www.ncbi.nlm.nih.gov/books/NBK9921/.

15. Vidal, Lara Sellés, et al. “Review of NAD(P)H-Dependent Oxidoreductases: Properties, Engineering and Application.” *Biochimica Et Biophysica Acta (BBA) - Proteins and Proteomics*, Elsevier, 10 Nov. 2017, www.sciencedirect.com/science/article/pii/S157096391730273X.